www.dergipark.gov.tr
ISSN:2148-3736

El-Cezerî Journal of Science and Engineering
Vol: 10, No: 1, 2023 (371-387)
DOI : 10.31202/ecjse.1225457

ECJSE

Research Paper

Development of Alkali-Activated Binders from Recycling Regional Tuff and Marble Wastes

İlker TEKİN[1a], Baraka CIZA[2b], H.S. GÖKÇE[3c,*]

[1]Department of Civil Engineering, Karabük University, Karabük, Türkiye
[2]The Graduate School of Natural and Applied Sciences, Dokuz Eylül University, İzmir, Türkiye
[3]Department of Civil Engineering, Bayburt University, Bayburt, Türkiye
[*]suleymangokce@bayburt.edu.tr

Received/Geliş: 28.12.2022 **Accepted/Kabul:** 25.05.2023

Abstract: The sustainability goals of the developing world have led many industries to recycle their wastes and reduce emitting greenhouse gases. To contribute to these environmental responsibilities, this study has focused on the development of eco-friendly binder materials from regional ground tuff and marble wastes by the activation of sodium silicate (Na_2SiO_3) and sodium hydroxide (NaOH) or slaked lime ($Ca(OH)_2$). The results of this study show that alkali-activated composites experienced expansion, drying shrinkage cracking, leaching, and efflorescence. The compressive strength values of the NaOH and $Ca(OH)_2$-activated pastes reached up to 15 MPa and 9 MPa, respectively. A reduction in NaOH molarity improved the compressive strength, dimensional stability, and durability of tuff-based alkali-activated pastes.

Keywords: Waste management, Waste disposal, Volcanic tuff, Marble wastes, NaOH activator, $Ca(OH)_2$ activator, Alkali-activated cements, Physical properties, Mechanical properties

1. Introduction

The cement industry being the second largest greenhouse gas emitter [1], is responsible for 8% of global anthropogenic CO_2 release [2]. The production of ordinary Portland cement which is the most common material used in the production of mortar, concrete, and other cementitious composites [3], results in the over-consumption of energy and natural resources [4]. The conservation of natural resources and environmental preservation can be achieved in the production of cement-based materials by partially replacing cement with by-products and wastes derived from power generation, timber manufacturing, iron and steelmaking, rice mill, mining industries, etc. [5, 6]. Much of these wastes can be recycled into making new products so as to reduce their detrimental effects on the environment [7]. Due to the ever-growing urbanization and the rapid development of industrialization these ever-increasing and harmful by-products and wastes can be advantageously used by partially replacing other raw materials in the production of new products [5]. Hereby, alkali-activated binders have recently become a popular research topic as an alternative to cement in material science and civil engineering [8-11].

Low calcium-based precursor materials are referred to as alkali-activated binders (AABs) while geopolymer binders (GBs) are high-calcium-based materials [12]. Van Deventer et al. [13] classified the binders ranging from Portland-based cement to geopolymers according to their chemistry variations. Recently, Gökçe et al. [14] have schematically expressed the classification of binding materials as seen in Figure 1. Geopolymers, a new class of three-dimensional inorganic polymers, could be synthesized from many silica and alumina-based materials with the reaction of an alkaline solution [15, 16]. In addition to aluminosilicate based-chemical composition, characteristics of

How to cite this article
Tekin İ., Ciza, B., Gökçe, H.S., "Development of Alkali-Activated Binders from Recycling Regional Tuff and Marble Wastes", El-Cezerî Journal of Science and Engineering, 2023, 10 (1); 371-387.
ORCID: [a]0000-0001-7400-4790; [b]0000-0001-9111-887X; [c]0000-0002-6978-0135

geopolymers are significantly varied by the fraction of glassy phase, soluble silicon, and aluminum, particle size distribution, presence of inert particles, particle morphology, and mineralogical structure [4]. Bhagath Singh and Subramaniam [17] have recently reported that the amount of alkaline solution and mechanical characteristics of the alkali-activated system are highly dependent on the reactive oxide fraction of the precursor.

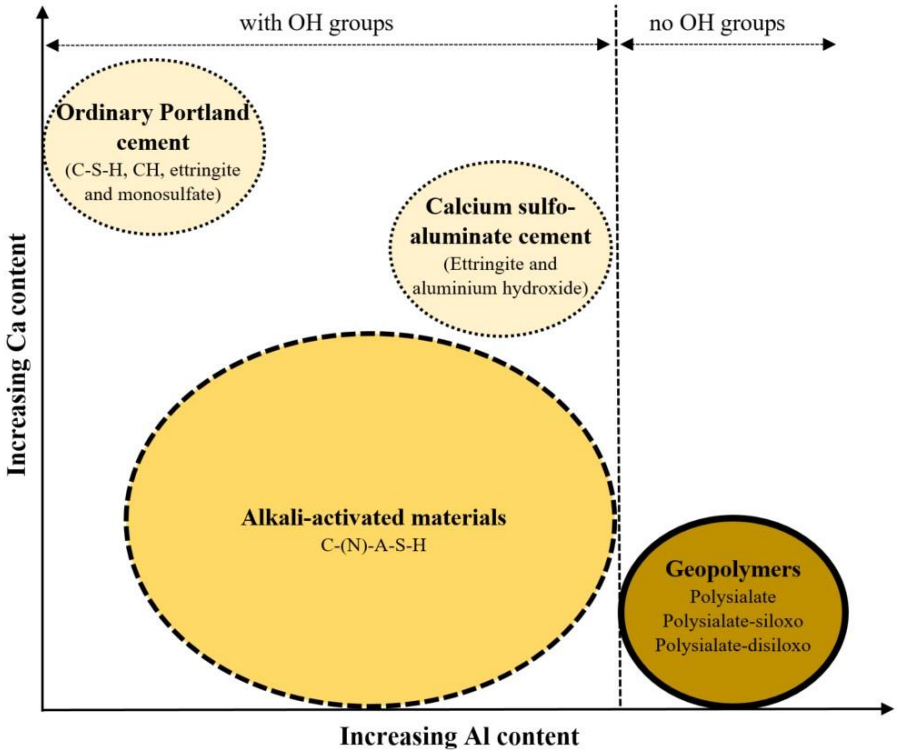

Figure 1. Classification of binders [14].

The development of AABs and GBs as an alternative to cement has provided an opportunity to utilize potential waste materials in commercial products [5, 18]. McLellan et al. [19] reported that geopolymer concrete mixtures could contribute to reducing greenhouse gases emission by up to 64% compared to those released from ordinary Portland cement concrete. Due to their rich aluminosilicate content, metakaolin [20], slag [21-23], bottom ash [24], rice husk ash [25, 26], bottom ash [27], fly ash [28-30] or their mixes [31-33] are the most preferred precursors in the production of alkali-activated and geopolymer systems.

As the availability of industrial by-products such as fly ash and slag fully depends on the production of their main products, natural aluminosilicate sources with lower footprints are becoming more and more popular in alkali-activated geopolymer systems [34]. Volcanic tuffs which are kinds of pozzolanic materials used in the cement industry are natural rich-aluminosilicate sources [35, 36]. Türkiye has rich natural resources of volcanic tuff [36] and marble stones [37] deserving the attention of researchers for their feasibility in the production of geopolymers and or AABs [38]. Marble wastes which are generated in great and ever-increasing quantities from quarries and workshops are rich in calcium oxide which poses a great threat to the environment and water if left unattended [38]. Thus, a great deal of recent research on making the most out of these wastes. Arel [39] have recently reported that wastes of marble stones could be recycled into cementitious systems with significant economic and ecological benefits. In their study, Saloni et al. [40] studied the effect of partially replacing natural aggregate with waste marble aggregate at various ratios ranging from 0 to 75% in fly ash-based alkali activated concrete. They concluded that replacing up to 50% natural aggregate with waste marble aggregates significantly improved mechanical properties such as compressive, flexural and split tensile strengths as well as the modulus of elasticity. Overall, they observed that the use of waste marble aggregate improved the pore structure through the densification of the

geopolymer matrix thanks to the formation of new polymeric and calcium-based products. Tammam et al. [41] studied the feasibility of waste filler materials and recycled waste aggregates on the development of geopolymer composites. They reported that the utilization of waste filler materials along with recycled aggregates successfully enhanced mechanical and durability properties of these composites.

As the waste portion of marble reaches up to 90% in quarrying and processing, marble producing-countries like China, Türkiye, Italy, Spain, and Greece encounter a huge amount of fine, block, and slab wastes that cause economic and environmental costs [42]. Hereby, these wastes of tuffs and marble are/can be recycled into the production of new materials.

Xu and van Defender [43] reported that many kinds of natural aluminosilicate minerals can be used to synthesize geopolymer materials having compressive strength values ranging between 2.5 Mpa and 18.9 Mpa by using KOH and NaOH as activators. These activators are alkaline solutions made by using alone or a combination of NaOH, KOH, Na_2SiO_3, $Ca(OH)_2$, and others [44]. According to a study conducted by Tekin [38], volcanic tuff wastes in combination with marble wastes were used to develop alkali-activated composites with 46-Mpa compressive strength at 90 days with the activation of 10 M NaOH solution alone. The use of NaOH and/or Na_2SiO_3 activators, as well as non-commercial zeolitic material could be utilized to synthesize geopolymers and alkali-activated materials [45, 46]. Djobo et al. [47] have recently produced volcanic ash based-geopolymer mortars having satisfactory strength and durability characteristics with the aid of Na_2SiO_3 and NaOH as activators. Volcanic ash-based systems need to be researched further due to the significant role of mineralogy and chemistry of volcanic ashes on geopolymerization and, consequently, on mechanical properties [16].

In this study, the effect of different alkaline activators with various molarity levels on setting time, water absorption, density, porosity, and compressive strength of waste-based alkali-activated pastes was investigated. Hence, the present study will contribute to the understanding of recycling potential of regional industrial wastes including volcanic tuff and marble dust, and to the development of eco-friendly binders for the production of specific construction materials.

2. Experimental Methods

2.1. Materials

In this study, tuff- and marble-based alkali-activated paste mixtures were produced by using sodium silicate, sodium hydroxide, and calcium hydroxide as activators. Volcanic tuff and marble wastes as presented in Figure 2 were collected from commercial regional production facilities in the Northeast of Türkiye. There are 3 kinds of tuffs in that region, which are found in colors of yellow, white, and green. Among them, yellow tuff is the most commonly used material in cladding tile production. Moreover, yellow tuff has the lowest hardness among the others. Therefore, 70% of stone waste arises from quarries. According to the mineralogical observation by the General Directorate of Mineral Research and Explorations (MTA), yellow tuff is derived from a matrix that has altered volcanic materials such as quartz, plagioclase, and stone particles. Calcite, feldspar, clay, pyroxene, and ferrite phases were observed in a fully altered matrix. Mineralogical and microscopic analyses are given in Figure 3 and Figure 4. According to the EDS analysis of Figure 3, clay- and silicate-based structures were found in the sample.

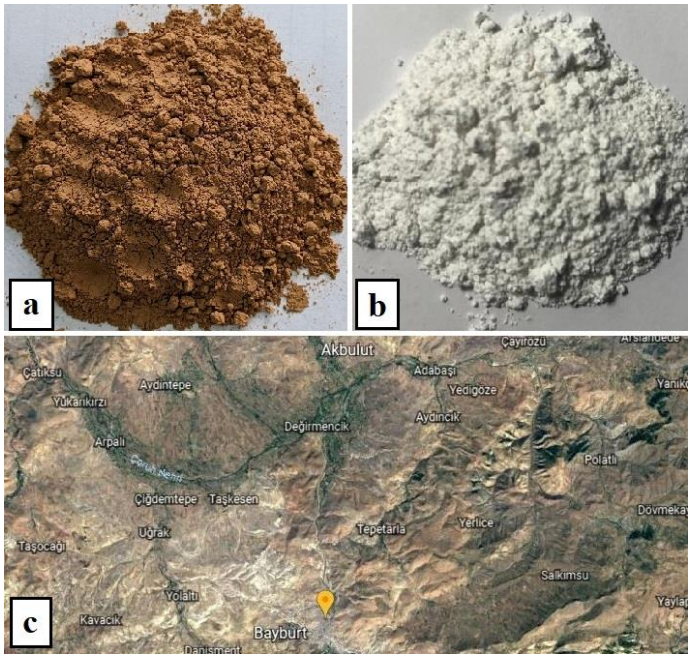

Figure 2. Volcanic tuff (a) marble dust (b) GPS coordinates 40.3318° N, 40.1438° E of the tuff location(c).

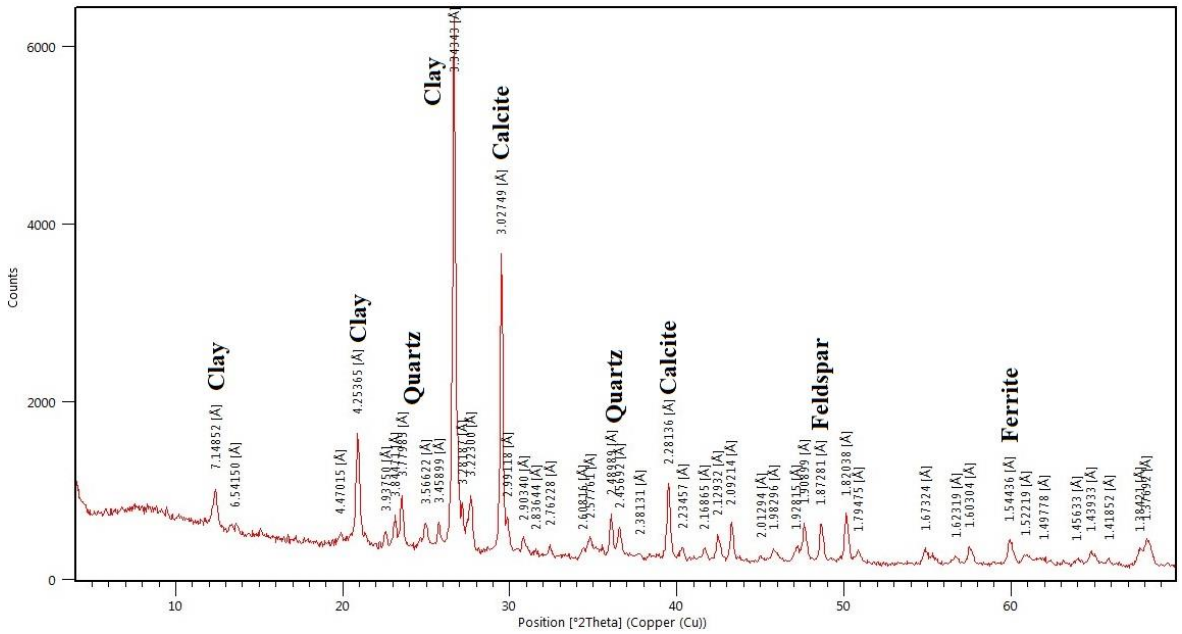

Figure 3. Mineralogical analyses of yellow tuff from northeast Türkiye.

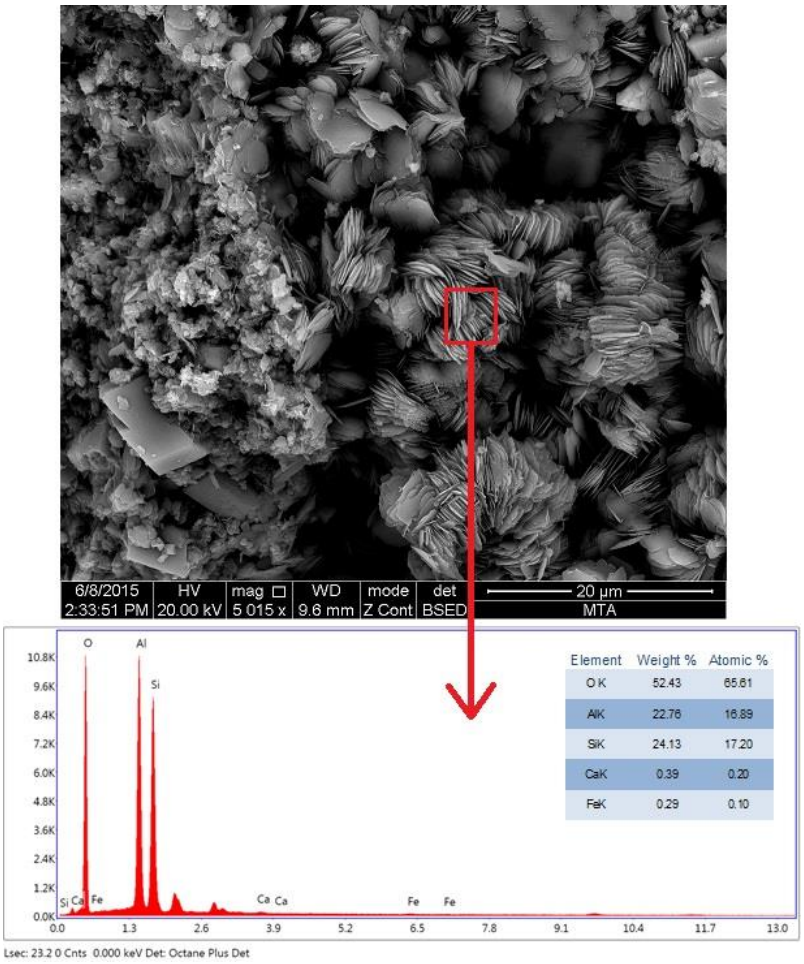

Figure 4. Microscopic analyses of yellow tuff from northeast Türkiye.

Particle size distribution of the ground tuff and marble wastes by using a ball mill is presented in Figure 5. 90% of the yellow tuff powder (TP) and marble dust (MD) were obtained by passing through 20- and 100-µm sieves, respectively. According to laser particle size analysis derived from Mastersizer 3000 instrument, it was determined that 70% and 45% ratios of the TP and MD particles were finer than 10 µm, respectively. The Blaine fineness of TP and MD was sequentially found to be 24220 cm^2/g and 2645 cm^2/g. The chemical composition of the materials is given in Table 1. TP was used as a precursor material thanks to its rich aluminosilicate content and smaller particle size, while the role of MD was designed to be a filler material in the matrix due to its lower fineness.

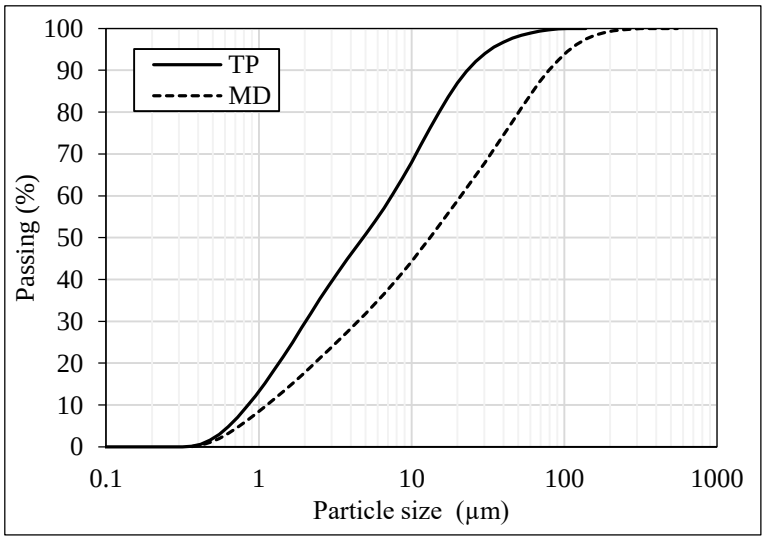

Figure 5. Particle size distribution of TPand MD.

Table 1. Oxide composition of TP and MD.

Oxides	TP	MD
SiO_2	70.37	0.70
Al_2O_3	11.01	-
Fe_2O_3	0.83	0.20
CaO	2.87	55.10
MgO	0.87	0.20
SO_3	0.15	-
Na_2O	1.36	-
K_2O	1.79	-
LOI	10.08	43.50
Total	99.33	99.70

Na_2SiO_3 solution (12% Na_2O + 24% SiO_2 + 64% H_2O) with 40-42 Baume value in aqueous solution at 20 °C was used. Pellet form NaOH with 99.9% purity, and calcium hydroxide with 98% purity were used as activators in the preparation of the alkaline mixing solutions.

2.2. Mix Proportions and Experimental Methods

In this experimental study, the mix proportions of alkali-activated pastes were determined by using the absolute volume method in order to achieve the best stoichiometric ratios based on prior knowledge from a previous study by Tekin [38]. In total, twelve mix series as seen in Table 2 were designed for the activation of TP with and without MD by using Na_2SiO_3 solution in the presence of NaOH or calcium hydroxide.

Table 2. Mix proportions and mix details.

Mix ID	Solid: 48% (by weight)			Liquid: 52% (by weight)		Liquid/solid material (by weight)	Na_2O (%)	Alkali concentration
	TP	MD	$Ca(OH)_2$	NaOH	Na_2SiO_3 Sol.			
N_h	0.48	-	-	0.16	0.36	1.1	16.7	High
N_m	0.48	-	-	0.14	0.38	1.1	15.4	Medium
N_l	0.48	-	-	0.12	0.40	1.1	14.1	Low
N_h-M	0.26	0.22	-	0.12	0.40	1.1	14.1	High
N_m-M	0.26	0.22	-	0.10	0.42	1.1	12.8	Medium
N_l-M	0.26	0.22	-	0.08	0.44	1.1	11.5	Low
C_h	0.24	-	0.24	-	0.52	1.1	N/A	High
C_m	0.25	-	0.25	-	0.50	1.0	N/A	Medium
C_l	0.26	-	0.26	-	0.48	0.9	N/A	Low
C_h-M	0.20	0.04	0.24	-	0.52	1.1	N/A	High
C_m-M	0.21	0.04	0.25	-	0.50	1.0	N/A	Medium
C_l-M	0.22	0.04	0.26	-	0.48	0.9	N/A	Low

* N/A: Solubility of $Ca(OH)_2$ at 20°C H_2O is 1.73 g/L, and molar mass $Ca(OH)_2$ is 74.05g/mol. Hence, the maximum concentration of $Ca(OH)_2$ solution that can be prepared at 20°C = 1.73g/L / 74.05g/mol = 0.023 mol/L. Since $Ca(OH)_2$ cannot be completely soluble in water, the molarity of $Ca(OH)_2$ solution cannot be argued in an alkali-activated systems. Therefore, the not applicable "N/A" term is used in this table.

A special mixing procedure was followed for the production of a homogenous alkali-activated paste matrix. In the NaOH-bearing series, an alkaline solution was prepared by dissolving solid pellets of NaOH in a Na_2SiO_3 solution. After cooling, the solution was mixed with TP for 45 secs at low speed (140 rpm). The mixing was elongated for 15 secs after MD addition. The final mixture was mixed for 30 secs at high speed (280 rpm). In $Ca(OH)_2$-bearing series, TP was mixed with Na_2SiO_3 solution for

30 secs at a low speed (140 rpm). In sequence, MD and $Ca(OH)_2$ with a 15 sec-interval were added to the mixture, and the mixing was carried out for 30 secs. The final mixture was stirred for 30 secs at high speed (280 rpm). The total time used for preparing every mixture used in this study was 2 min. The prepared mixtures were cast into 50-mm cube molds. After resting at the laboratory condition (20±2 °C and 50% relative humidity), the specimens were removed from the molds. While NaOH-bearing series were cured at 50% relative humidity in the laboratory at 20±2 °C, $Ca(OH)_2$-bearing series were kept in wet condition until 2 and 28 days when the compressive strength test was performed. The tailored-curing procedure of the alkali-activated systems is required to avoid leaching and cracking of the specimens from drying shrinkage.

The standard consistency and setting time of the alkali-activated pastes were tested by following the procedures described in ASTM C187-16 [48] and ASTM C191-13 [49]. At constant dispersing Newtonian media, the workability of suspension systems is highly affected by the volume, particle size distribution and morphology of the solid particles in them. Hence, to make sure that all mixes possessed equal workability, standard consistency tests with the help of a vicat apparatus were performed in a series of trial and error. As a result, only mixes of normal consistency were selected for use. The 2 and 28-day compressive strengths were determined by the average result of 3 specimens for each series in accordance with ASTM C109/C109M-02 [50]. Oven-dry density and water absorption of the composites were determined according to ASTM C642-06 [51]. In addition, the apparent porosity of the samples was calculated by using Equation (1). Furthermore, the determination of specific gravity (SG) was carried out by using Le Chatelier flask as in [38]. Lastly, visual inspection as well as tape measuring at 2 and 28-day of curing were sought for in assessing dimensional stability of samples.

$$P = SG \times w \quad (1)$$

where P: apparent porosity (%), SG: apparent specific gravity of specimen, w: water absorption by weight (%).

3. Results and Discussion

Cartwright et al. [52] reported that when compared to ordinary Portland cement (OPC), alkali-activated binders are prone to higher total shrinkage values possibly caused by drying, chemical activation, and carbonation. Furthermore, at ambient conditions (25 °C and 50% RH), the drying shrinkage of alkali-activated systems can reach up to 3 times higher that of OPC [53]. In this study, the appearance of the demolded specimens (after 24 h) are given in Figure 6a and 6b for NaOH- and $Ca(OH)_2$-activated pastes, respectively. Cracks caused by drying shrinkage were more pronounced in $Ca(OH)_2$-bearing mixtures, while enough (sufficient) dimensional stability was achieved in NaOH-activated pastes. Häkkinen [54] reported long ago that the cracking is caused by the pore characteristics of alkali-activated systems. According to Gökçe and Tuyan [55], such cracks formations could be sufficiently reduced in geopolymer systems by the introduction of aggregate and the replacement of high Ca-bearing precursor material (Class C fly ash) with low Ca-bearing ones (Class F fly ash).

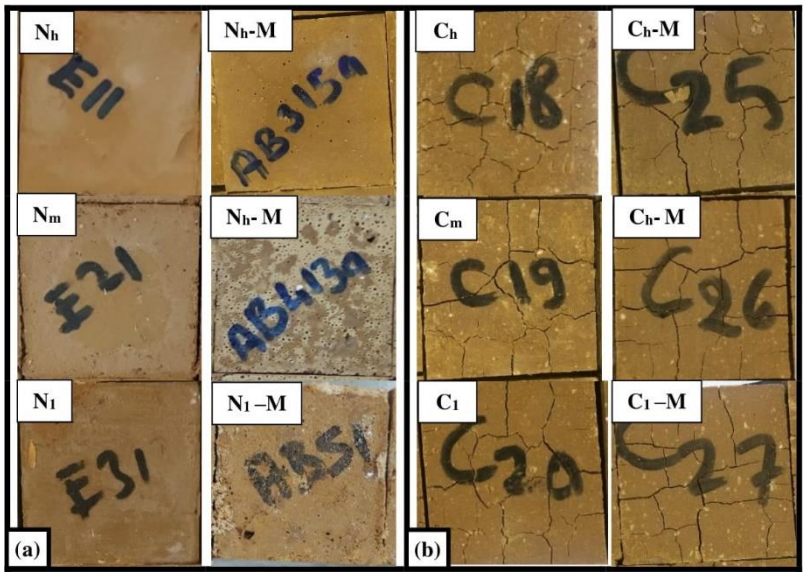

Figure 6. Appearances of hardened (a) NaOH- and (b) $Ca(OH)_2$-activated pastes after 24 h.

3.1. Setting Time

The initial and final setting time values are presented in Figures 7a and 7b for NaOH- and $Ca(OH)_2$-activated pastes, respectively. The values are basic characteristics of hydraulic binders for determining the workability duration of produced mortar and concrete composites. As shown in Figure 7a, the presence of MD led to the decrease in setting time of NaOH-activated pastes at high and medium alkali concentrations. While the initial setting time values ranged between 4 min. and 45 min., the final setting time values were between 15 min. and 60 min. The setting time values significantly decreased in $Ca(OH)_2$-activated pastes. In general, the durations decreased to 8 min. for the initial setting and down to 37 min. for the final setting (Figure 7b). This can be identified as a flash set characteristic which is a well-known phenomenon in cementitious systems. Such binder properties can be desired for tailored-construction materials and industrial productions such as repair mortars and precast members. Furthermore, the setting times were found to be dramatically affected by the molarity of NaOH in exception of the final setting times for mixes without MD. As the molarity of NaOH within pastes decreases, setting times values increase and vice versa. This can be attributed to the fast dissolution of alumina silicate structures because of the higher pH values of the solution. Moreover, SiO_2, Al_2O_3, and CaO-based formations become quickly formed in the presence of higher NaOH content. In the absence of MD, there were no significant changes observed in the final setting times of NaOH-based samples. In fact, the core of these samples remained wet even after 2 days of curing. It is thought that at high alkali concentration a strong barrier forms around the TP particles slowing down their reaction and the formation of the hydrates leading to longer final setting times.

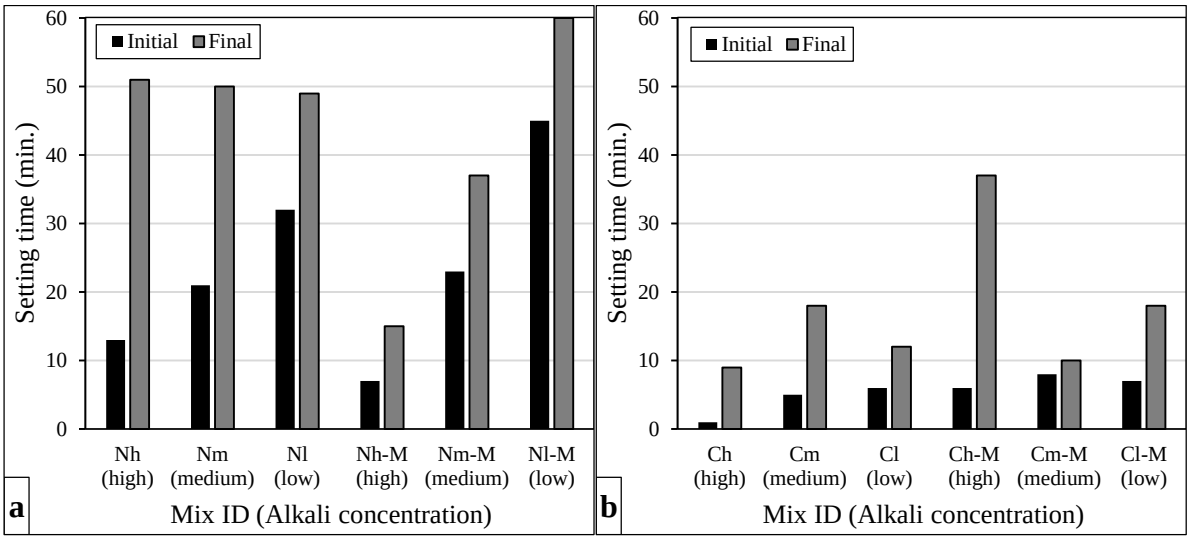

Figure 7. Initial and final setting time values of (a) NaOH- and (b) $Ca(OH)_2$-activated mixtures.

Marble is mainly formed of calcite, or crystalline calcium carbonate [56]. The presence of calcite allows the formation of thermodynamically more stable carbonate phases from sulfoaluminate products, while it acts as an inert filler [57]. Hereby, the reactive characteristic of MD will contribute to the activation of aluminosilicate-based sources, and accelerate the setting time values. Similarly, Tekin [38] reported that the introduction of MD accelerated the setting time values of NaOH-activated geopolymers. The presence of free CaO in activators can reduce the setting time of the geopolymer systems further [34].

3.2. Water Absorption and Porosity

In performing the water absorption and porosity test, the specimens were severely damaged during the keeping in water and oven. In general, NaOH-activated specimens were degraded in water as seen in Figure 8a, while the drying process in an oven at 105±5 °C disintegrated the $Ca(OH)_2$-activated specimens as shown in Figure 8b.

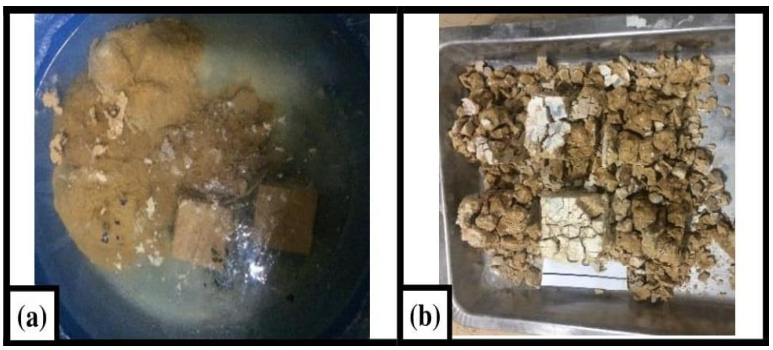

Figure 8. Degradation of (a) NaOH-activated specimens in water and (b) $Ca(OH)_2$-activated specimens after oven drying.

Table 3 presents water absorption, oven-dry density and porosity results of the 28-day alkali-activated specimens. The porosity levels ranging from 50.2 to 53.6% are found to be significantly higher compared to results previously obtained (from 14.5 to 22.6%) from a study performed by Gökçe et al. [58]. The highly porous structure contributes to the density decrement of hardened specimens down to 1014 kg/m^3 in this study. According to Haga et al. [59], this study presents almost similar porosity (51.6%) and density (≈1050 kg/m^3) as hydrated cement paste produced with a 0.8 of w/c ratio.

Table 3. Physical characteristics of alkali activated specimens.

Mix ID	Liquid/solid (by weight)	Water absorption (%)	Density (kg/m^3)	Porosity (%)
N_h	1.1	-	-	-
N_m	1.1	49.6	1058	52.5
N_l	1.1	47.9	1111	53.2
N_h-M	1.1	-	-	-
N_m-M	1.1	-	-	-
N_l-M	1.1	-	-	-
C_h	1.1	52.5	1014	53.3
C_m	1.0	49.8	1054	52.5
C_l	0.9	47.0	1083	50.9
C_h-M	1.1	52.0	1030	53.6
C_m-M	1.0	48.4	1060	51.2
C_l-M	0.9	45.0	1114	50.2

A good linear relationship (see Figure 9) was founded between the liquid-to-solid ratio and porosity of $Ca(OH)_2$-activated mixtures. The increment in the liquid-to-solid ratio resulted in slightly higher porosity for these specimens. This finding broadly supports the work of previous studies in this area linking the increase in L/S ratio with porosity increment [60]. In their study, Marczyk et al. [60] reported that the density of geopolymers decreased with increase in L/S ratio. Similarly, Jaya et al. [61] observed that there is a loss in compressive strength with increase in L/S ratio. This can be explained by the formation of a lesser dense aluminosilicate matrix. In other words, the increase in L/S ratio engenders large interparticle distances resulting in large pores left unfilled by the hydration products [61]. Marczyk et al. [60] explained that it could also be related to the condensation effect that occurs during the polymerization reaction. Furthermore, the increment in porosity for $Ca(OH)_2$-based specimens can also be attributed to severe drying shrinkage cracks. As reported by Gökçe et al. [58] remarkable porosity increments can cause significant strength loss in alkali-activated and geopolymer binders. On the other hand, such high-volume porosity characteristics cause severe leaching potential, high density, and strength loss in even hardened cement pastes [59].

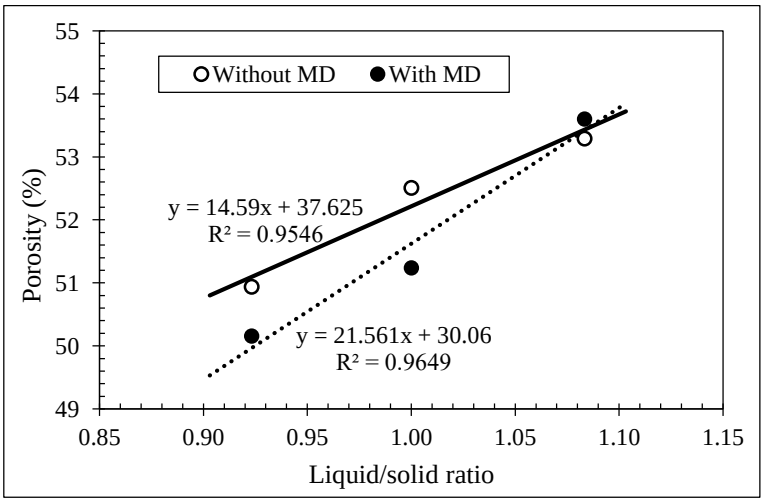

Figure 9. Relation between liquid-to-solid ratio and porosity for $Ca(OH)_2$-activated specimens.

3.3. Compressive Strength

The 2- and 28-day compressive strength values are given in Figure 10a and 10b for NaOH- and $Ca(OH)_2$-activated pastes, respectively. The introduction of MD and reduction in alkaline molarity remarkably improved the compressive strength of NaOH-activated pastes. The ultimate (28-d) compressive strength of $Ca(OH)_2$-activated pastes reduced in presence of MD while there are

negligible variations in 2-day compressive strength results. There is no clear effect of alkaline molarity on the 2- and 28-day compressive strength values of $Ca(OH)_2$-activated pastes. When compared to the compressive strength values of NaOH-activated specimens reaching up to 14.6 MPa, the lower compressive strength values of $Ca(OH)_2$-activated mixtures reaching up to 9.0 MPa are possibly caused by severe crack formations on hardened specimens.

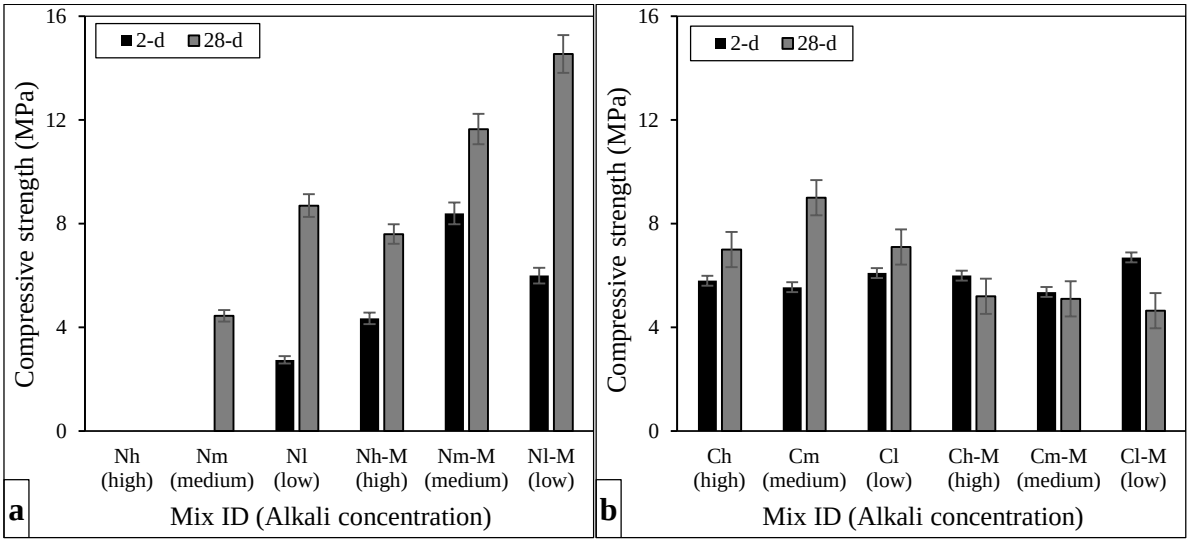

Figure 10. 2- and 28-day compressive strength values of (a) NaOH- and (b) $Ca(OH)_2$-activated mixtures.

After the testing of compressive strength, core parts of the tested NaOH-activated specimens were found to be wet, the observed inner core wetness was especially in higher percentages for specimens with high alkaline activator. The high barrier quality of alkali aluminosilicate hydrate gels formed in outer parts of specimens blocks the release of some water involved in reactions [62], which explains the reason some NaOH-activated specimens of this study were found to have no or very low compressive strength values after 2 days. Moreover, the unexpected decrement in the compressive strength results was mainly caused by the deterioration of the specimens due to longer curing times. Furthermore, the incorporation of MD in NaOH-activated specimens led to the increase in compressive strength at both 2 and 28-day. For instance, with the introduction of MD there occurred strength increments of about 120% and 65% for sample Nl (without MD) and Nl-M (with MD), after 2 and 28 days respectively. The same trend was observed for all other samples albeit at different ratios. Furthermore, it has been observed that MD introduction greatly improved the dimensional stability of NaOH-activated specimens. The increase in strength with MD introduction can be attributed to the formation of additional calcium-based products that led to the densification of the matrix through the refinement of pores. Jindal et al [63] explained that despite MD not bearing pozzolanic properties, in presence of an alkaline solution, the CaO in its structure may react with this solution to form additional CSH, CASH and NASH. As for $Ca(OH)_2$-based it was observed that the compressive strength of these samples decreased at 28 days to become slightly lower than that of 2 days. The most plausible reason is thought to be the severity of shrinkage cracks experienced by these samples especially at 28 days. Similar results were reported by Tammam et al [41] who suggested that the presence of MD in $Ca(OH)_2$-based AABs could led to the generation of excessive heat of hydration which gives way to severe cracking of samples impeding the formation of a dense and homogenous matrix. In The presence of MD, the pore structures (Figure 11a) of NaOH-based specimens were found to be significantly smaller than those (Figure 11b) of $Ca(OH)_2$-based specimens at 28 days. Therefore, the smaller pore structure expresses the reason for the higher compressive strength results found in NaOH-based specimens exposed to prolonged curing.

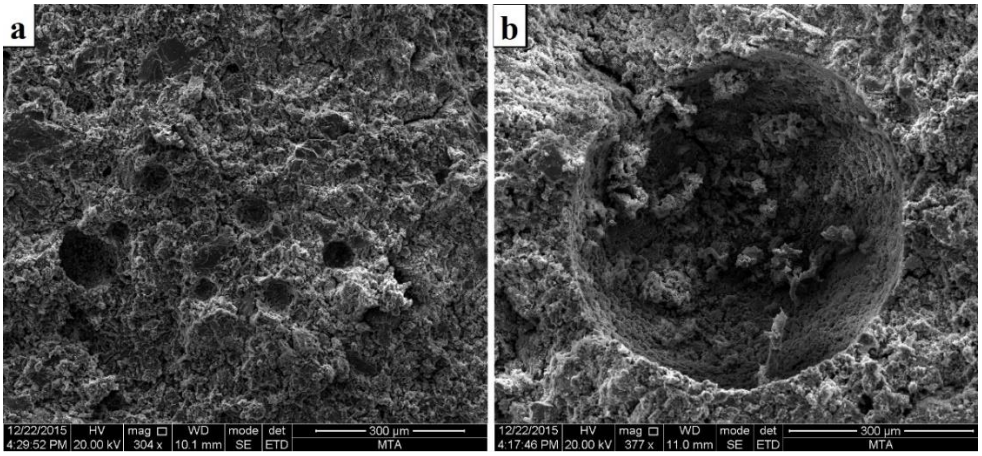

Figure 11. Pore structure of (a) NaOH-based and (b) $Ca(OH)_2$-based specimens.

Some deteriorations which are observed as severe efflorescence and crack propagation (see Figure 12a and 12b) softened the hardened NaOH- and $Ca(OH)_2$-activated specimens, thus reducing their mechanical properties. The efflorescence formation was gradually deteriorating with an increment of; alkaline molarity content for NaOH-activated mixtures, and relative humidity for $Ca(OH)_2$-activated mixtures.

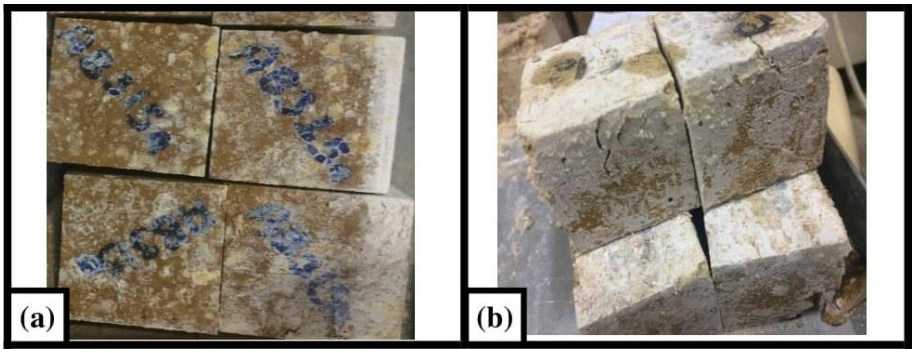

Figure 12. Deterioration of (a) NaOH- and (b) $Ca(OH)_2$-activated specimens.

High pH level caused by high alkali concentrations reduces the solubility of CaO, and interrupts its bonding with NaO. So, the free NaO tends to lead to the carbonation of specimens, especially at deleterious amounts in high alkaline mixtures. Due to the higher volume, the dried alkali carbonates cause an expansion and reduction in the compressive strength of alkali-activated pastes [64]. The dimensional stability of the NaOH-activated specimens is very poor in elongated curing time. The 2-day (Figure 13a) and 28-day appearances (Figure 13b) of a specimen show that the NaOH-activated systems have poor volumetric stability.

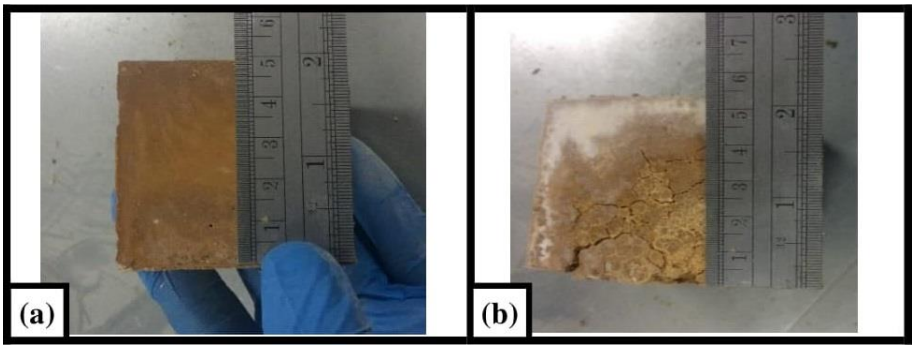

Figure 13. (a) 2- and (b) 28-d appearances of a NaOH-activated specimen (Nh).

The oxide compositions and certain constants of the alkali-activated mixtures are presented in Table

4 in order to understand the geopolymerization kinetics.

Table 4. The oxide compositions (XRF) of 28-d specimens.

Oxide fractions	N_h	N_m	N_l	N_h-M	N_m-M	N_l-M	C_h	C_m	C_l	C_h-M	C_m-M	C_l-M
SiO_2	28.2	28.8	29.4	42.5	43.0	43.4	27.4	27.5	27.6	29.8	30.1	30.4
Al_2O_3	2.8	2.8	2.8	5.2	5.3	5.2	2.2	2.3	2.5	2.6	2.8	2.9
Fe_2O_3	0.3	0.3	0.3	0.4	0.4	0.4	0.2	0.2	0.2	0.2	0.2	0.2
CaO	12.8	12.8	12.8	1.4	1.4	1.4	2.5	2.6	2.8	0.7	0.7	0.8
MgO	0.3	0.3	0.3	0.4	0.4	0.4	0.2	0.2	0.2	0.2	0.2	0.2
SO_3	0.0	0.0	0.0	0.1	0.1	0.1	0.0	0.0	0.0	0.0	0.0	0.0
Na_2O	17.6	15.5	13.3	21.4	19.6	17.9	30.4	31.3	32.3	30.4	31.4	32.3
K_2O	0.5	0.5	0.5	0.9	0.9	0.9	0.4	0.4	0.4	0.4	0.4	0.5
LOI	37.3	38.8	40.4	27.5	28.7	30.0	36.6	35.3	33.8	35.5	34.0	32.5
SiO_2/Al_2O_3	10.0	10.2	10.4	8.1	8.2	8.3	12.3	11.8	11.2	11.4	10.9	10.5
Na_2O/Al_2O_3	6.2	5.5	4.7	4.1	3.7	3.4	13.6	13.4	13.1	11.6	11.4	11.2
SiO_2/Na_2O	1.6	1.9	2.2	2.0	2.2	2.4	0.9	0.9	0.9	1.0	1.0	0.9
Na_2O/Al_2O_3	6.2	5.5	4.7	4.1	3.7	3.4	13.6	13.4	13.1	11.6	11.4	11.2
CaO/SiO_2	0.5	0.4	0.4	0.032	0.032	0.031	0.1	0.1	0.1	0.023	0.024	0.025

The design of geopolymer systems in SiO_2/Na_2O ratio of 1.5 is important to exhibit lower porosity, higher density, and strength [65]. Although the present study is of similar SiO_2/Na_2O ratios, the other constants remarkably deteriorate the satisfactory strength results. In this respect, Zhang et al. [66] recommended the SiO_2/Al_2O_3 of 4.5 and the Na_2O/Al_2O_3 of 0.8 to improve the strength of geopolymer systems. As seen from Table 4, the Al_2O_3 content of the systems is insufficient. Thus, the geopolymerized structures could not be formed completely in the present study due to the selection of a poor aluminosilicate source (TP). On the other hand, the presence of high CaO contributes to the cementitious gels and densifies the microstructures by filling the pores from inert parts of it in early curing periods. Acceleration of setting time and early strength gain of the $Ca(OH)_2$-activated specimens are caused by the aforementioned phenomena.

4. Conclusions

Global and regional diversity force many researchers to find locational and tailored solutions contributing to the responsibilities and sustainability goals of the modern construction industry. An effort was made to develop an alkali-activated binder from regional volcanic tuff and marble wastes in the current study. The following conclusions can be drawn from the setting time, porosity and compressive strength results of these alkali-activated binders:

- The $Ca(OH)_2$ activator remarkably accelerated the setting time of these binders compared to NaOH. The variation allows the use of binders in tailored fields. NaOH-activated binders can be used in an in-situ application while $Ca(OH)_2$-activated binders are recommended in the precast industry. However, the final setting time values (for NaOH-activated binders: 60 min. and $Ca(OH)_2$-activated binders: 37 min.) are still short compared to that of cement counterparts.
- The alkali-activated materials produced mainly from volcanic materials were found to be significantly porous (porosity: 50.2%≤) and lighter (density: ≤1114 kg/m^3) structures. The increment of the liquid-to-solid ratio increased the porosity up to 53.6% and decreased the density down to 1014 kg/m^3. There were found good linear relations (R2: 0.96≤) between the liquid-to-solid ratio and porosity of $Ca(OH)_2$-activated pastes.
- The introduction of MD led to the refining of the pore structure for NaOH-based samples. Whereas for $Ca(OH)_2$-based samples, it gave way to severe shrinkage cracks and higher permeability.
- The NaOH activator was found more suitable for the strength development of alkali-activated systems compared to the $Ca(OH)_2$ activator. Waste marble dust introduction improved the compressive strength of the NaOH-activated mixtures up to 14.6 MPa. The ultimate (28-day) compressive strength of $Ca(OH)_2$-activated mixtures was found remarkably lower (reduced from 9.0

MPa to 4.7 MPa) in presence of marble dust. In addition, the introduction of marble dust slightly softened the 2-day $Ca(OH)_2$-activated specimens at 28 days.

- In conclusion, the authors of the present study recommend the $NaOH+Na_2SiO_3$ activation for the blending of volcanic tuff and marble dust obtained from regional wastes in low alkaline concentrations to produce an alternative alkali-activated binder material having enough volumetric stability, drying shrinkage, leaching and efflorescence potential.

Authors' Contributions

İT designed the conceptualization of the study. BC carried out the experimental works with the collaboration and advice of İT, wrote the original draft and proofread and revised this paper. HSG wrote the paper. HSG and İT are the overall supervisors of the study.

All authors have read and approved the final version of the manuscript.

Competing Interests

The authors declare that they have no competing interests.

References

[1]. Sumesh, M., Alengaram, U. J., Jumaat, M. Z., Mo, K.H. and Alnahhal, M. F., "Incorporation of nano-materials in cement composite and geopolymer based paste and mortar – A review", Constr. Build. Mater., 2017, 148: 62-84.
[2]. Andrew, R. M., "Global CO_2 emissions from cement production, 1928–2017", Earth Syst. Sci. Data, 2018, 10: 2213-2239.
[3]. Bhutta, A., Farooq, M., Zanotti, C. and Banthia, N., "Pull-out behavior of different fibers in geopolymer mortars: effects of alkaline solution concentration and curing", Mater. Struct., 2017, 50: 80.
[4]. Zhang, P., Zheng, Y., Wang, K. and Zhang, J., "A review on properties of fresh and hardened geopolymer mortar", Compos. Part B Eng., 2018, 152: 79-95.
[5]. Ng, C., Alengaram, U. J., Wong, L. S., Mo, K. H., Jumaat, M. Z. and Ramesh, S., "A review on microstructural study and compressive strength of geopolymer mortar, paste and concrete", Constr. Build. Mater., 2018, 186: 550-576.
[6]. Kolawole, J. T., Olusola, K. O., Babafemi, A. J., Olalusi, O. B. and Fanijo, E., "Blended cement binders containing bamboo leaf ash and ground clay brick waste for sustainable concrete", Materialia, 2021, 15: 101045.
[7]. Espuelas, S., Echeverria, A. M., Marcelino, S., Prieto, E. and Seco, A., "Technical and environmental characterization of hydraulic and alkaline binders", J. Clean. Prod., 2018, 196: 1306-1313.
[8]. Provis, J. L., "Alkali-activated materials", Cem. Concr. Res., 2018, 114: 40-48.
[9]. Shwekat, K. and Wu, H.-C. "Benefit-cost analysis model of using class F fly ash-based green cement in masonry units", J. Clean. Prod., 2018, 198: 443-451.
[10]. Adesina, A. "Performance of fibre reinforced alkali-activated composites – A review", Materialia, 2020, 12: 100782.
[11]. Kaze, C. R., Tome, S., Lecomte-Nana, G. L., Adesina, A., Essaedi, H., Das, S. K., Alomayri, T., Kamseu, E. and Melo, U. C., "Development of alkali-activated composites from calcined iron-rich laterite soil", Materialia, 2021, 15: 101032.
[12]. Provis, J. L., "Geopolymers and other alkali activated materials: why, how, and what?", Mater. Struct., 2013, 47: 11-25.

[13]. van Deventer, J. S. J., Provis, J. L., Duxson, P. and Brice D. G., "Chemical research and climate change as drivers in the commercial adoption of alkali activated materials", Waste Biomass Valori., 2010, 1: 145-155.
[14]. Gökçe, H. S., Tuyan, M. and Nehdi, M. L., "Alkali-activated and geopolymer materials developed using innovative manufacturing techniques: A critical review", Constr. Build. Mater., 2021, 303: 124483.
[15]. Andrejkovičová, S., Sudagar, A., Rocha, J., Patinha, C., Hajjaji, W., Ferreira da Silva, E., Velosa, A. and Rocha, F., "The effect of natural zeolite on microstructure, mechanical and heavy metals adsorption properties of metakaolin based geopolymers", Appl. Clay Sci., 2016, 126: 141-152.
[16]. Djobo, J. N. Y., Elimbi, A., Tchakouté, H. K., and Kumar, S., "Volcanic ash-based geopolymer cements/concretes: the current state of the art and perspectives", Environ. Sci. Pollut. Res. Int., 2017, 24: 4433-4446.
[17]. Bhagath Singh, G. V. P. and Subramaniam, K. V. L., "Effect of active components on strength development in alkali-activated low calcium fly ash cements", Journal of Sustainable Cement-Based Materials, 2019, 8: 1-19.
[18]. Krishna, R. S., Mishra, J., Zribi, M., Adeniyi, F., Saha, S., Baklouti, S., Shaikh, F. U. A. and Gökçe, H. S. "A review on developments of environmentally friendly geopolymer technology", 2021, Materialia 20: 101212.
[19]. McLellan, B. C., Williams, R. P., Lay, J., van Riessen, A. and Corder, G. D., "Costs and carbon emissions for geopolymer pastes in comparison to ordinary portland cement", J. Clean. Prod., 2011, 19: 1080-1090.
[20]. Clausi, M., Tarantino, S. C., Magnani, L. L., Riccardi, M. P., Tedeschi, C. and Zema, M., "Metakaolin as a precursor of materials for applications in Cultural Heritage: Geopolymer-based mortars with ornamental stone aggregates", Appl. Clay Sci., 2016, 132-133: 589-599.
[21]. Sethi, H., Bansal, P. P. and Sharma, R., "Effect of addition of GGBS and glass powder on the properties of geopolymer concrete", Iran J. Sci. Technol. Trans. Civ. Eng., 2019, 43: 607–617.
[22]. Bingöl, Ş., Bilim, C., Atiş, C. D. and Durak, U., "Durability properties of geopolymer mortars containing slag", Iran J. Sci. Technol. Trans. Civ. Eng., 2020, 44: 561–569.
[23]. Khater, H. M. and Abd el Gawaad, H. A., "Characterization of alkali activated geopolymer mortar doped with MWCNT", Constr. Build. Mater., 2016, 102: 329-337.
[24]. Hanjitsuwan, S., Phoo-ngernkham, T. and Damrongwiriyanupap, N., "Comparative study using Portland cement and calcium carbide residue as a promoter in bottom ash geopolymer mortar", Constr. Build. Mater., 2017, 133: 128-134.
[25]. Kim, Y. Y., Lee, B. J., Saraswathy, V. and Kwon, S.-J., "Strength and durability performance of alkali-activated rice husk ash geopolymer mortar", Sci. World J., 2014, 2014: 209584.
[26]. Nimwinya, E., Arjharn, W., Horpibulsuk, S., Phoo-Ngernkham, T. and Poowancum, A., "A sustainable calcined water treatment sludge and rice husk ash geopolymer", J. Clean. Prod., 2016, 119: 128-134.
[27]. Xie, T. and Ozbakkaloglu, T., "Behavior of low-calcium fly and bottom ash-based geopolymer concrete cured at ambient temperature", Ceram. Int., 2015, 41: 5945-5958.
[28]. Adak, D., Sarkar, M. and Mandal, S., "Structural performance of nano-silica modified fly-ash based geopolymer concrete", Constr. Build. Mater., 2017, 137: 430-439.
[29]. Assi, L., Ghahari, S., Deaver, E., Leaphart, D. and Ziehl, P., "Improvement of the early and final compressive strength of fly ash-based geopolymer concrete at ambient conditions", Constr. Build. Mater., 2016, 123: 806-813.
[30]. Gunasekara, C., Law, D. W. and Setunge, S., "Long term permeation properties of different fly ash geopolymer concretes", Constr. Build. Mater., 2016, 124: 352-362.
[31]. Pilehvar, S., Cao, V. D., Szczotok, A. M., Carmona, M., Valentini, L., Lanzón, M., Pamies, R. and Kjøniksen, A.-L., "Physical and mechanical properties of fly ash and slag geopolymer concrete containing different types of micro-encapsulated phase change materials", Constr. Build. Mater., 2018, 173: 28-39.

[32]. Nana, A., Epey, N., Rodrique, K. C., Deutou, J. G. N., Djobo, J. N. Y., Tomé, S., Alomayri, T. S., Ngouné, J., Kamseu, E. and Leonelli, C., "Mechanical strength and microstructure of metakaolin/volcanic ash-based geopolymer composites reinforced with reactive silica from rice husk ash (RHA)", Materialia, 2021, 16: 101083.
[33]. Sharmin, A., Alengaram, U. J., Jumaat, M. Z., Yusuf, M. O., Kabir, S. M. A. and Bashar, I. I., "Influence of source materials and the role of oxide composition on the performance of ternary blended sustainable geopolymer mortar", Constr. Build. Mater., 2017, 144: 608-623.
[34]. Firdous, R., Stephan, D. and Djobo, J. N. Y., "Natural pozzolan based geopolymers: A review on mechanical, microstructural and durability characteristics", Constr. Build. Mater., 2018, 190: 1251-1263.
[35]. Liebig, E. and Althaus, E., "Pozzolanic activity of volcanic tuff and suevite: Effects of calcination", Cem. Concr. Res., 1998, 28: 567-575.
[36]. Türkmenoğlu, A. G. and Tankut, A., "Use of tuffs from central Turkey as admixture in pozzolanic cements: Assessment of their petrographical properties", Cem. Concr. Res., 2002, 32: 629-637.
[37]. Çelik, M. Y. and Sabah, E., "Geological and technical characterisation of Iscehisar (Afyon-Turkey) marble deposits and the impact of marble waste on environmental pollution", J. Environ. Manage., 2008, 87: 106-116.
[38]. Tekin, I., "Properties of NaOH activated geopolymer with marble, travertine and volcanic tuff wastes", Constr. Build. Mater., 2016, 127: 607-617.
[39]. Arel, H. Ş., "Recyclability of waste marble in concrete production", J. Clean. Prod., 2016, 131: 179-188.
[40]. Lim YY, Pham TM, Kumar J., "Sustainable alkali activated concrete with fly ash and waste marble aggregates: Strength and Durability studies", Constr. and Build. Mater., 2021, 283:122795.
[41]. Tammam Y, Uysal M, Canpolat O, Kuranlı ÖF., "Effect of Waste Filler Materials and Recycled Waste Aggregates on the Production of Geopolymer Composites", Arab J Sci Eng., 2022 Sep 9:1-8.
[42]. Altun, N. E., "Assessment of marble waste utilization as an alternative sorbent to limestone for SO_2 control", Fuel Process. Technol., 2014, 128: 461-470.
[43]. Xu, H. and van Deventer, J. S. J., "The geopolymerisation of alumino-silicate minerals", Int. J. Miner. Process, 2000, 59: 247-266.
[44]. de Vargas, A. S., Dal Molin, D. C. C., Masuero, Â. B., Vilela, A. C. F., Castro-Gomes, J. and de Gutierrez, R. M., "Strength development of alkali-activated fly ash produced with combined NaOH and $Ca(OH)_2$ activators", Cem. Concr. Compos., 2014, 53: 341-349.
[45]. Villa, C., Pecina, E. T., Torres, R. and Gómez, L., "Geopolymer synthesis using alkaline activation of natural zeolite", Constr. Build. Mater., 2010, 24: 2084-2090.
[46]. Pekgöz, M., Tekin, İ., "The effects of different origins NaOH on the mechanical and microstructural properties of tuff-based alkali-activated pastes", Turkish Journal of Engineering Research and Education, 2022, 1: 29-37.
[47]. Djobo, J. N. Y., Elimbi, A., Tchakouté, H. K. and Kumar, S., "Mechanical properties and durability of volcanic ash based geopolymer mortars", Constr. Build. Mater., 2016, 124: 606-614.
[48]. ASTM C187-16, Standard Test Method for Amount of Water Required for Normal Consistency of Hydraulic Cement Paste, ASTM International, West Conshohocken, PA, (2016).
[49]. ASTM C191-13, Standard Test Methods for Time of Setting of Hydraulic Cement by Vicat NeedleASTM International, West Conshohocken, PA, (2018).
[50]. ASTM C109/C109M-02, Standard Test Method for Compressive Strength of Hydraulic Cement Mortars (Using 2-in. or (50-mm) Cube Specimens)ASTM International, West Conshohocken, PA, (2017).
[51]. ASTM C642-06, Standard Test Method for Density, Absorption, and Voids in Hardened ConcreteASTM International, West Conshohocken, PA, (2013).

[52]. Cartwright, C., Rajabipour, F. and Radlińska, A., "Shrinkage characteristics of alkali-activated slag cements", J. Mater. Civ. Eng., 2015, 27: B4014007.
[53]. Collins, F. and Sanjayan, J., "Effect of pore size distribution on drying shrinking of alkali-activated slag concrete", Cem. Concr. Res., 2000, 30: 1401-1406.
[54]. Häkkinen, T., "The influence of slag content on the microstructure, permeability and mechanical properties of concrete Part 1 Microstructural studies and basic mechanical properties", Cem. Concr. Res., 1993, 23: 407–421.
[55]. Gökçe, H. S. and Tuyan, M., "Effect of mix design parameters on crack intensity of fly ash-based geopolymer mortar with high-volume paste", 3rd International Conference on Civil and Environmental Engineering, İzmir, Turkey (2018).
[56]. Corinaldesi, V., Moriconi, G. and Naik, T. R., "Characterization of marble powder for its use in mortar and concrete", Constr. Build. Mater., 2010, 24: 113-117.
[57]. Matschei, T., Lothenbach, B. and Glasser, F. P., "The role of calcium carbonate in cement hydration", Cem. Concr. Res., 2007, 37: 551-558.
[58]. Gökçe, H. S., Tuyan, M., Ramyar, K. and Nehdi, M. L., "Development of eco-efficient fly ash-based alkali-activated and geopolymer composites with reduced alkaline activator dosage", J. Mater. Civ. Eng., 2020, 32: 04019350.
[59]. Haga, K., Sutou, S. and Hironaga, M., "Effects of porosity on leaching of Ca from hardened ordinary Portland cement paste", Cem. Concr. Res., 2005, 35: 1764-1775.
[60]. Marczyk J, Ziejewska C, Pławecka K, Bąk A, Łach M, Korniejenko K, Hager I, Mikuła J, Lin WT, Hebda M. "Optimizing the L/S Ratio in Geopolymers for the Production of Large-Size Elements with 3D Printing Technology", J. Mater., 2022, 15(9):3362.
[61]. Xu Z, Yue J, Pang G, Li R, Zhang P, Xu S. Influence of the activator concentration and solid/liquid ratio on the strength and shrinkage characteristics of alkali-activated slag geopolymer pastes. Advances in Civil Engineering. 2021 Feb 9;2021:1-1.
[62]. Matalkah, F., Salem, T., Shaafaey, M. and Soroushian, P., "Drying shrinkage of alkali activated binders cured at room temperature", Constr. Build. Mater., 2019, 201: 563-570.
[63]. Jindal BB, Parveen, Singhal D, Goyal A., "Predicting relationship between mechanical properties of low calcium fly ash-based geopolymer concrete", Trans. Indian Ceram. Soc., 2017, 76(4):258-65.
[64]. Ortega-Zavala, D. E., Santana-Carrillo, J. L., Burciaga-Díaz, O. and Escalante-García, I., "An initial study on alkali activated limestone binders", Cem. Concr. Res., 2019, 120: 267-278.
[65]. Gao, K., Lin, K. and Wang, D., "Effects SiO_2/Na_2O molar ratio on mechanical properties and the microstructure of nano-SiO_2 metakaolin-based geopolymers", Constr. Build. Mater., 2014, 53: 503-510.
[66]. Zhang, Y., Sun, W. and Li, Z., "Composition design and microstructure characterization of geopolymer binder", J. Chin. Ceram. Soc., 2008, 36(S1): 153-159.